NOTES AND CORRESPONDENCE

The Three-Dimensional Axisymmetric Wind Field Structure of the Spencer, South Dakota, 1998 Tornado

KAREN KOSIBA AND JOSHUA WURMAN

Center for Severe Weather Research, Boulder, Colorado

ABSTRACT

The three-dimensional axisymmetric wind field structure of the violent Spencer, South Dakota, 1998 tornado was analyzed using the ground-based velocity track display (GBVTD) method. Data from a Doppler on Wheels mobile radar, collected at very close range to the tornado, were used to conduct the GBVTD calculations at a very fine (16 m) resolution. The analysis revealed a two-cell vortex with a very strong axial downdraft throughout the observation period, radial inflow jets preceding intensification and a decrease in inflow preceding weakening, swirl ratio values consistent with observed multiple vortex structure, and other features of the vortex.

1. Introduction

Laboratory (e.g., Ward 1972; Davies-Jones 1973, 1976; Church et al. 1979; Church and Snow 1993) and numerical (e.g., Rotunno 1977, 1979, 1984; Lewellen and Sheng 1980; Gall 1983; Walko 1988; Fiedler 1993; Fiedler and Rotunno 1986; Howells et al. 1988; Lewellen et al. 1997, 2000; Lewellen and Lewellen 2007a,b) models of tornado-like vortices depict a wide range of possible vortical flows. Each of these regimes has an associated vortex structure and velocity distribution, which greatly impact the surface wind field. For example, the strongest velocities are hypothesized to occur upstream of a vortex breakdown (the transition region between supercritical and subcritical flow regimes) because of the inability of the vortex to fill in from aloft. Depending on the height of the vortex breakdown, these intense velocities can occur aloft or very near the surface. Other vortical flow structures, such as single-celled, two-celled, and multiple vortices, are also possible (Fig. 1). These flow regimes are, of course, complicated by a multitude of interactions that are not included in most laboratory and numerical models. In particular, the effects of surface roughness, large-scale inhomegeneities such as terrain, and thermodynamics on vortex structure are not well known. Further, the relationship between tornado structure and damage incurred at the surface remains largely undocumented.

Mobile radars (e.g., Bluestein and Unruh 1993; Bluestein et al. 1995; Wurman et al. 1997; Bluestein and Pazmany 2000; Wurman 2001; Wurman et al. 2008) have been pivotal in providing high-resolution, near-surface data of tornadoes. While mobile radars have observed over 150 tornadoes in total (Alexander and Wurman 2008), nearly all of these observations have been conducted with a single radar. Rarely have simultaneous finescale, suitably arranged, and synchronized observations of tornadoes been obtained with multiple mobile radars (e.g., Richardson et al. 2001; Dowell et al. 2002; Wurman et al. 2007a,b; Marquis et al. 2008; Wurman et al. 2010). None of the aforementioned dual-Doppler observations had adequate resolution to resolve adequately tornado-scale features. Although mapping of tornadoes using just single-Doppler observations has been conducted (e.g., Wurman et al. 1996a; Wurman and Gill 2000; Wurman 2002; Bluestein et al. 2004; Alexander and Wurman 2005, hereafter AW05; Wurman and Alexander 2005, hereafter WA05; Bluestein et al. 2007), these studies have suffered from the inability to measure the two- or three-dimensional vector wind field directly, which is possible with multiple radars. Consequently, there has been much effort to reconstruct the vector wind fields of tornadoes
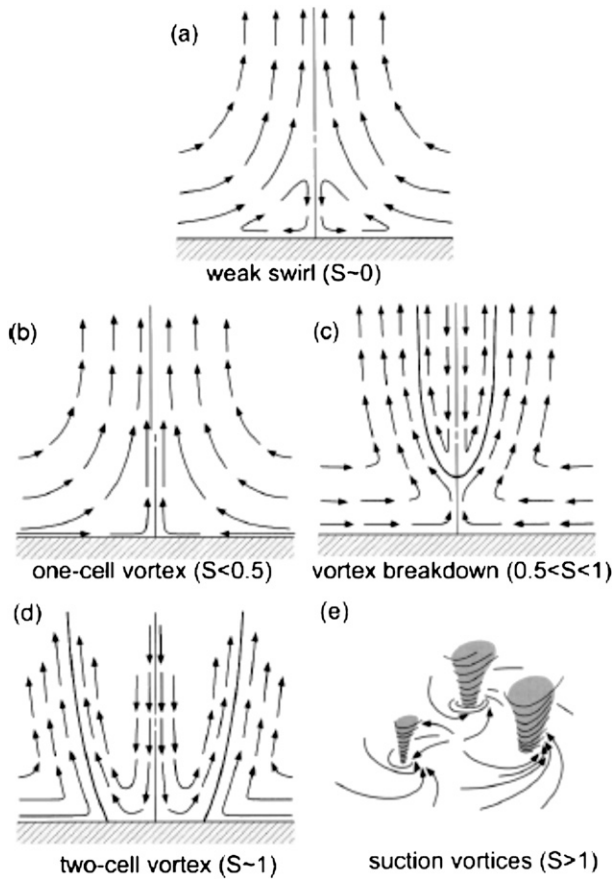
FIG. 1. Idealized vortex structures as a function of swirl ratio. Adapted from Davies-Jones (1986). Vertical cross sections are shown in (a)–(d).
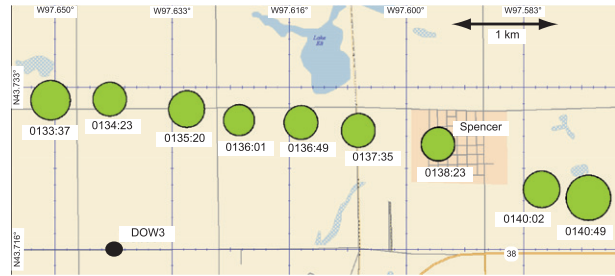

FIG. 2. The track of the Spencer, South Dakota, 1998 tornado as determined from DOW3 data (location of DOW3 marked with black circle). The green disks indicate the area within the radius of maximum winds as determined from DOW3 data.

from single-Doppler data. In two cases (Bluestein et al. 2003; Tanamachi et al. 2007) only two-dimensional wind fields have been retrieved. Up until now, full three-dimensional vector wind fields have only been retrieved from single-Doppler data in two tornadoes: the Mulhall, Oklahoma, tornado of May 1999 and the Harper, Kansas, tornado of May 2004 (Lee and Wurman 2005, hereafter LW05; Kosiba et al. 2008, hereafter KTW08).

Using the ground-based velocity track display (GBVTD) technique of Lee et al. (1999), LW05 documented the two-celled structure of the Mulhall, Oklahoma, tornado. They found that the tornado maintained a two-celled and/ or multiple vortex structure throughout the observation period. The depth of the inflow approached 600 m, but the strongest inflow was confined to very near the surface. Using the assumption of axisymmetry, KTW08 diagnosed the structure of the Harper, Kansas, tornado. They found that changes in the flow immediately surrounding the tornado vortex corresponded to differences in vortex structure and intensity. As in LW05, surges in low-level radial inflow were followed by increases in tornado intensity.

Additionally, both analyses revealed tangential velocity profiles that approximated a modified Rankine vortex. The two-dimensional analysis of Tanamachi et al. (2007) revealed divergent flow inside of the radius of maximum winds, implying a two-celled structure at the observation level, as the Stockton, Kansas, tornado reached peak intensity. Unfortunately data were only available at one level, so changes in vortex intensity could not be linked to changes in low-level inflow.

Given the paucity of three-dimensional analyses, the purpose of this study is to detail the evolution of the three-dimensional structure and associated dynamics of the 30 May 1998 Spencer, South Dakota, tornado. As the three-dimensional structure of a tornado has only been diagnosed twice prior to this work, comparisons between the three-dimensional features observed in this tornado to those observed in the Mulhall, Oklahoma (LW05), and Harper, Kansas (KTW08), tornadoes are made in order to ascertain which relationships and features persist and are repeatable through independent observations in different tornadoes.

2. Methodology and description of the data

The Doppler on Wheels 3 (DOW3) mobile radar collected data from approximately 0100 to 0145 UTC 31 May 1998 during a tornadic event that caused F4 damage in the town of Spencer, South Dakota (AW05). The tornado formed at approximately 0104 UTC and was in the dissipating stage when the DOW3 radar ceased operations at 0145 UTC. This paper focuses on the tornado structure between 0133 and 0140 UTC, during which time the tornado transected the town of Spencer (Fig. 2) and was continuously observed by the DOW. During this analysis interval, the distance to the center of the tornado from the DOW ranged from 1.7 to 6.5 km, yielding a 0.5° elevation observation altitude of approximately 20 m AGL when the tornado was at its closest approach to the DOW. A gate spacing of 37 m was used and the DOW

half-power beamwidth ranged from 28 to 106 m during the study period, which was oversampled by a factor of approximately 2, resulting in azimuthal sample spacing of 14–53 m. Nine volume scans, approximately one every 45 s, were completed from very near the ground [$O(\sim 20$ m$)$] to several hundred meters aloft. The number of levels in a volume varied between 5 and 10, with a finest angle increment of 0.5° and a coarsest angle increment, between the highest radar sweeps, of 3.0°. Data were dealiased and ground clutter was removed before analysis. A detailed discussion of the data postprocessing can be found in AW05.

To investigate the axisymmetric three-dimensional structure of the tornado, the ground-based velocity track display (Lee et al. 1999) technique was employed.

DOW data were interpolated to a Cartesian grid ($\Delta x = \Delta y = 16$ m, $\Delta z = 40$ m) using a bilinear interpolation scheme (Mohr et al. 1986). Although the analysis grid was chosen to be finer than the radar grid resolution in order to oversample the axisymmetric winds, the overall resolution of the analysis was limited by the radar measurements. To facilitate the mapping of the three-dimensional structure using the GBVTD technique, the center of the tornado circulation at each level was shifted so that the centers were stacked vertically. The data were then transferred to a tornado-centric grid at 16-m annuli. Nine volumes of DOW data, from 0133:37 to 0140:49 UTC (hereafter all times reference the beginning of the volume), were used in the analysis. The core flow region of the tornado was over Spencer during two of these volumes, 0138:23 and 0139:14 UTC.

Figure 3 depicts example radar scans at 1.4° for each of the volumes used in the analysis. Initially, at 0133:37 UTC, a peak Doppler velocity of 83 m s^{-1} at 23 m AGL characterized the low-level circulation. The tornado intensified slightly to 88 m s^{-1} and then maintained a relatively steady intensity until 0136:49 UTC when a peak Doppler wind of 104 m s^{-1} was reached (Fig. 4a). After 0136:49 UTC, the tornado remained relatively intense with peak Doppler winds exceeding 90 m s^{-1} until 0140:49 UTC, when the peak winds began to wane. The Doppler velocity structure between 0133:37 and 0140:49 UTC appeared highly asymmetric. Indeed, AW05 attribute oscillations in delta-V (the difference in magnitude between maximum inbound and outbound Doppler velocities) during this time to evidence of multiple vortices, and possibly modulation in the damage pattern (WA05). Unfortunately, because of the rather small diameter of the Spencer, South Dakota, tornado compared to the resolution of the DOW measurements (at a range of 4 km, the DOW beamwidth was over 60 m), higher wavenumber perturbations, which were spatially much smaller than the basic axisymmetric flow structure,

could not be extracted accurately from the GBVTD analysis.

3. The axisymmetric structure

The time evolution of the axisymmetric horizontal winds as a function of radius at 40 m AGL is depicted in Fig. 5a. Initially, from 0133:37 to 0136:49 UTC, there was strong radial flow into the tornado at 40 m AGL, penetrating inward to a radius of 200–300 m. Radial inflow exceeded 10 m s^{-1} outside a radius of 500 m from 0133:37 to 0136:58 UTC. The inflow then weakened after 0136:58 UTC, decreasing by over 60% between 0136:58 and 0137:45 UTC. There was very little low-level inflow throughout the rest of the analysis period. These values are consistent with the analyses of LW05 and KTW08, who reported maximum inflow values of 23 and 20 m s^{-1}, respectively, in the lowest retrieval level, underscoring that there can be significant inflow very near the surface. The importance of this inflow will be discussed subsequently in the context of vortex intensification. Outflow, also typically exceeding 10 m s^{-1} at 40 m AGL, persisted from very near the tornado centerline to a radius of approximately 200 m at the beginning of the analysis and gradually expanded outward with time. Although it is difficult to resolve the winds very close to the centerline, the overall radial wind distribution suggested a two-celled vortex structure. This two-celled structure persists throughout the analysis. The strongest horizontal gradient of the radial winds was just outside of the radius of maximum winds (RMW); thus, the maximum axisymmetric tangential winds occurred just inside the updraft/downdraft interface.

At the lowest analysis level (40 m AGL), the axisymmetric tangential winds peaked at 0134:23 UTC, waned until 0136:49 UTC, and then increased until 0138:23 UTC when the maximum axisymmetric tangential winds reached a peak of 79 m s^{-1} (Fig. 4a). After 0138:23 UTC, the axisymmetric tangential winds decreased to approximately 70 m s^{-1}. The 40-m axisymmetric RMW fluctuated about 200 m throughout the analysis, but there was an indication of broadening in the last volume at 0140:49 UTC (Fig. 4b) coincident with a decrease in tornado intensity (as measured by the peak Doppler winds and the peak axisymmetric tangential winds). A comparison between the axisymmetric RMW and the RMW ascertained from the raw Doppler data (WA05) revealed a greater fluctuation in size and consistently smaller radius in the radar-derived RMWs than in the radii retrieved from the GBVTD technique. The difference is usually less than 50 m, which is the beamwidth of the DOW at about 3-km range. Some of the difference may also be due in part to the presence of multiple
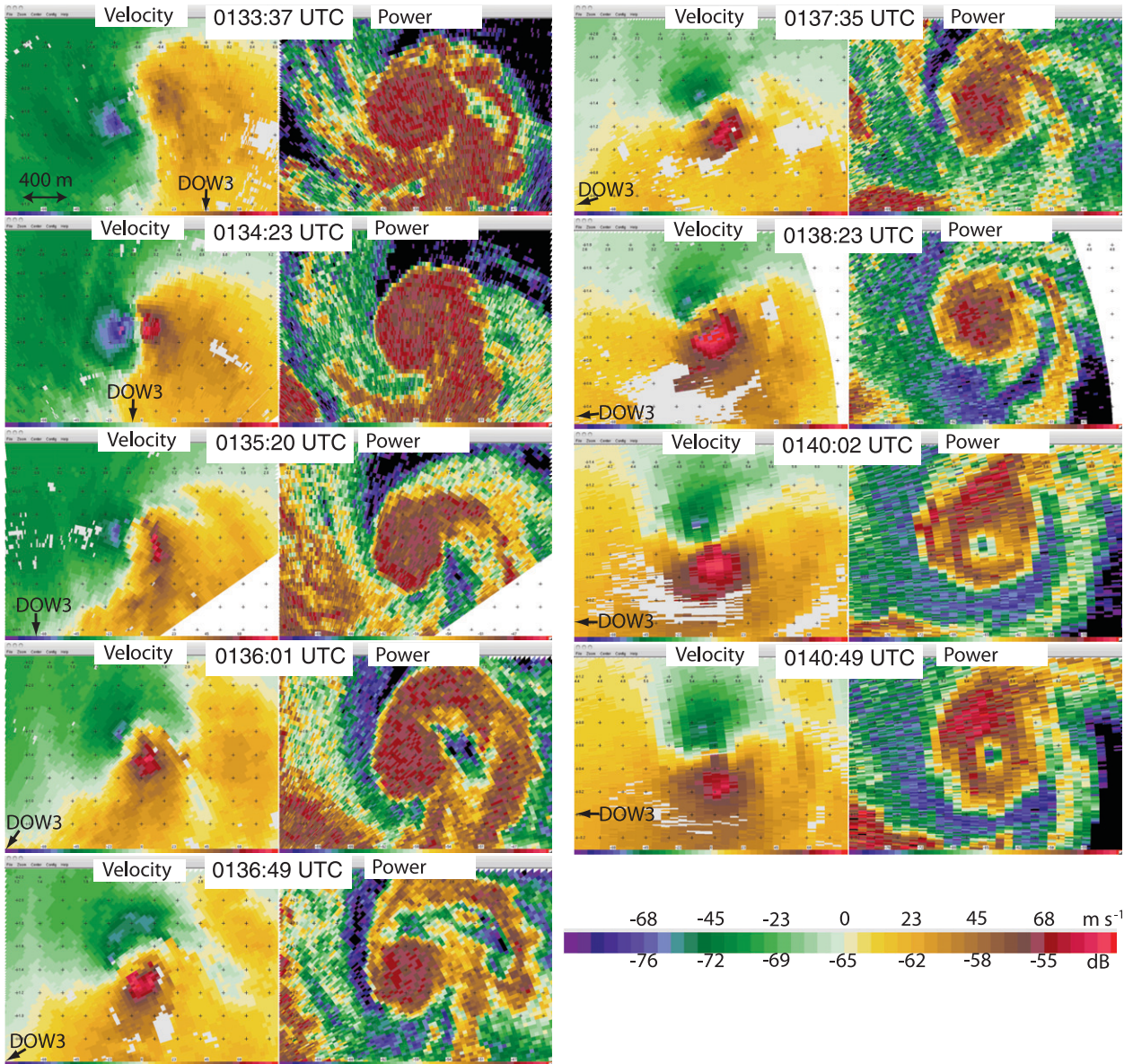
FIG. 3. The evolution of the Doppler velocity and received power in the tornado during the GBVTD analysis period. Shown are (left) Doppler velocity and (right) radar reflectivity; the location of DOW3 is indicated with an arrow.

vortices, which could contain several velocity maxima, making it difficult to subjectively determine the radius. Similar to LW05 and Tanamachi et al. (2007), the RMW and the maximum tangential winds were inversely related.

Aloft, at 400 m AGL (Fig. 5b), radial inflow of lesser magnitude than at 40 m, which peaked at about 10 m s^{-1} but typically had values of 5–10 m s^{-1}, persisted throughout the majority of the analysis. In the last couple of volumes, however, weak outflow was present at 400 m AGL. The near-axis radial flow was complicated by changes in the vortex structure, which will be discussed later.

Tangential winds at 400 m were generally weaker than those at 40 m AGL, and the maximum tangential winds were always lower at 400 m AGL compared to 40 m AGL. However, there were exceptions such as beyond 500-m radius where 400-m AGL tangential winds were more intense. It is hypothesized that this larger swath of stronger winds at 400 m AGL is characteristic of the two-celled vortex structure, which expands radially outward with height.

The Hovmöller diagrams present a two-dimensional time evolution of the winds at particular altitudes. It is also useful to examine the corresponding changes in the
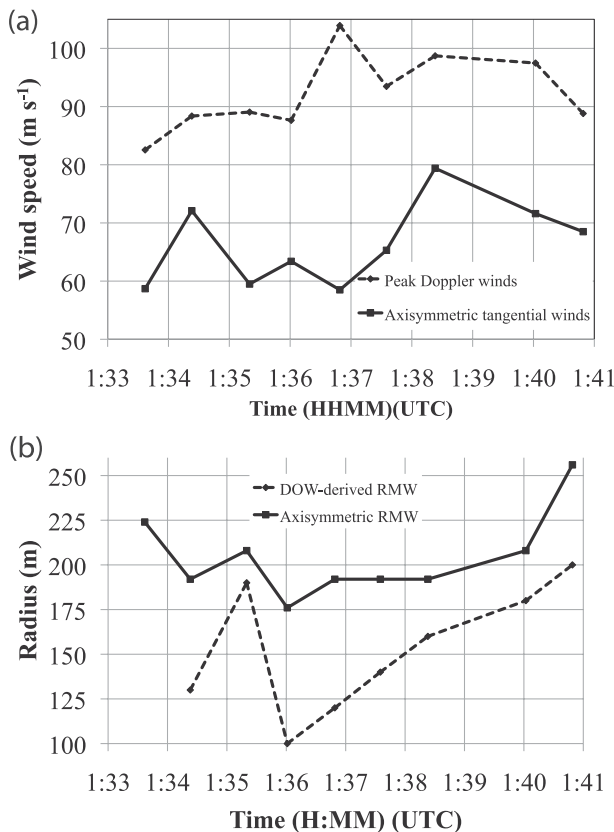
FIG. 4. Evolution of the Doppler velocity couplet and axisymmetric wind speed couplet. (a) Peak Doppler winds and axisymmetric tangential winds. (b) RMW from raw Doppler data and RMW from GBVTD axisymmetric wind field retrieval.

FIG. 5. Axisymmetric tangential winds (shading, m s^{-1}) and radial winds (contours) as a function of time and radius at (a) 40 and (b) 400 m AGL.

vertical structure of the tornado vortex. At 0133:37 UTC, the tornado appeared to have a fully two-celled structure throughout the depth of the analysis domain (Fig. 6). The general structure was remarkably unchanging throughout the analysis period. During the 7-min analysis period, the tornado exhibited a two-cell structure. This is in contrast to the rapidly changing structure observed in the Dimmitt (1995; Wurman and Gill 2000) and Harper (2004; KTW08) tornadoes, and the rapid structural changes observed in the Kellerville (1995) tornado (Wurman et al. 1997). Tangential winds are weaker at 0135:20 UTC, a time associated with apparent multiple vortex structure in the raw Doppler data (Wurman 2002). Tangential winds peak at 0138:23 UTC, just as the tornado core flow begins to impinge on the town of Spencer. The maximum downdraft existed aloft and very near the central axis, approaching 60 m s^{-1} at $z = 800$ m. Note that the precise magnitude of the retrieved vertical velocity values should be viewed with caution. Even with the lowest-level DOW scans approaching 15 m AGL, near-surface convergence may not be well resolved. Unresolved convergence would spuriously increase the
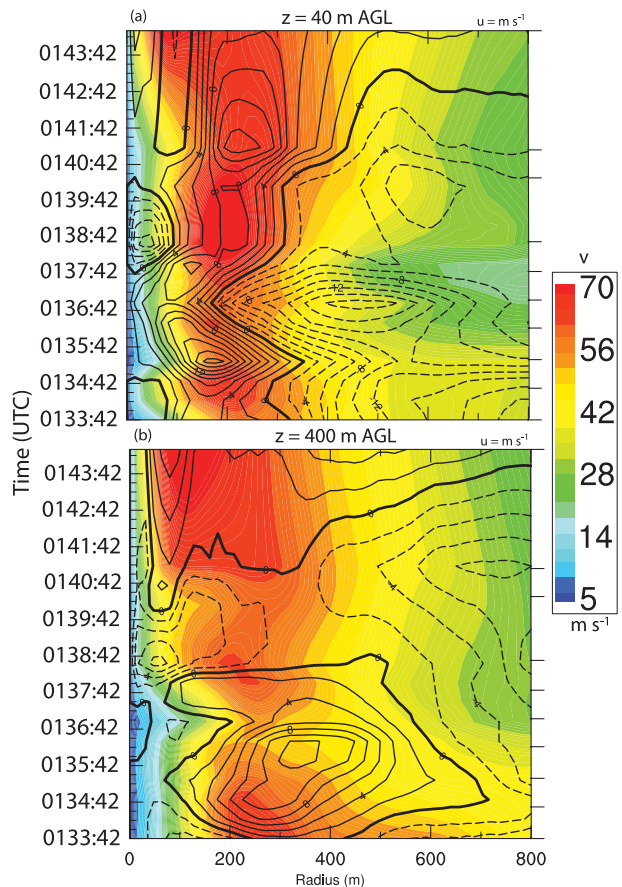
magnitude of calculated downdrafts. And, given the rather coarse observations, it is likely that the on/near-axis processes were not well resolved, leading to erroneous or aliased retrievals. Therefore, while it was likely that an intense central downdraft existed, the magnitude of this feature was likely ill represented. This fully two-celled structure persisted throughout the analysis interval. A 60 m s^{-1} downdraft was considerably stronger than the ∼30 m s^{-1} downdrafts estimated in the Dimmitt, Texas, tornado (Wurman et al. 1996a; Wurman and Gill 2000) and the Mulhall, Oklahoma, tornado (LW05). However, Fiedler and Rotunno (1986) have suggested that downdrafts of this or even stronger intensities are possible in two-celled tornadoes. At certain retrieval times—0135:20, 0136:49, and 0138:23 UTC in particular—there are closed circulations at about 300 m AGL. These may be related to the multiple vortex structure observed at these times, but they may also be artifacts of the retrieval process.

Initially, at 0133:37 UTC, the near-surface tangential winds were weaker than the winds aloft. By the next
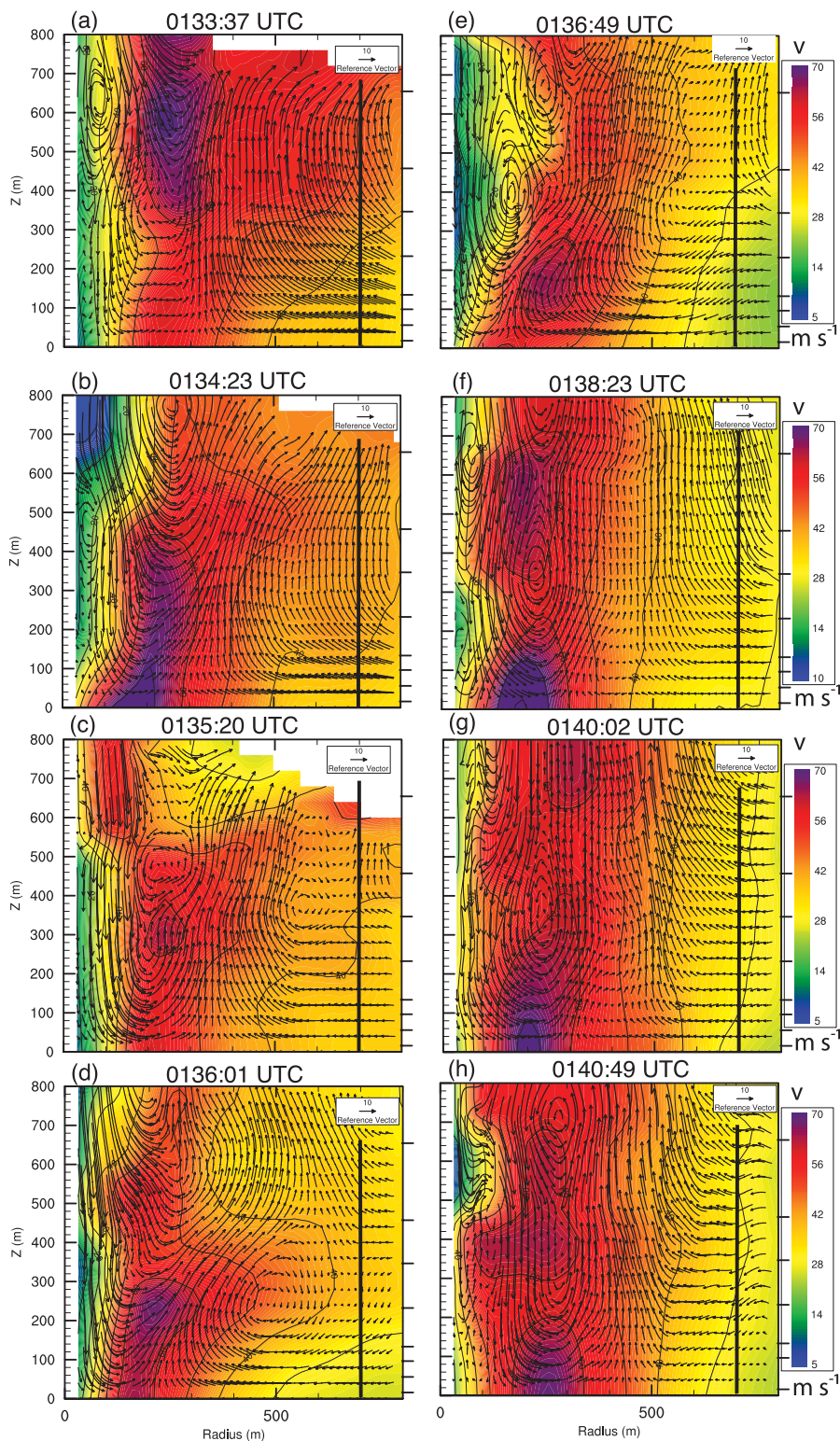
FIG. 6. Axisymmetric structure (radius–height) of the tornado at each analysis time. The secondary circulation (vectors) and the tangential winds (shading) are shown from 0133:37 to 0140:49 UTC. During this time, the tornado retains a fully two-celled structure during intensification and demise. The vertical black line indicates $r = 700$ m.
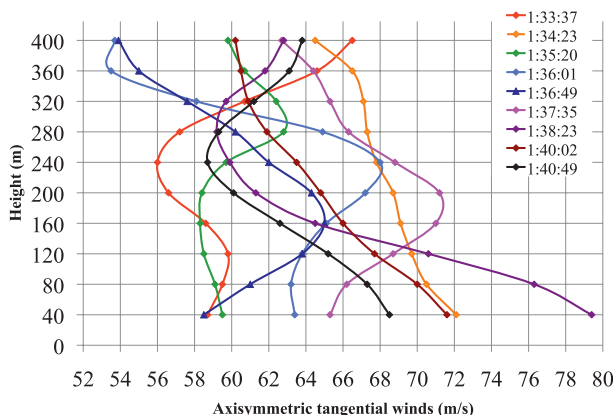
FIG. 7. Axisymmetric maximum tangential winds as a function of height from 0135:20 to 0140:49 UTC. The largest axisymmetric tangential velocities occur in the lowest analysis level at 0134:23, 0138:23, 0140:02, and 0140:49 UTC.
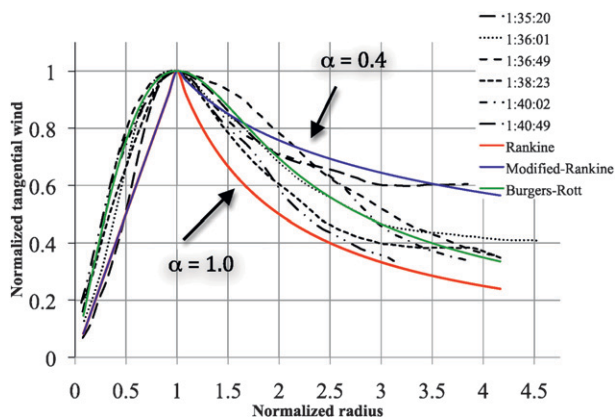

FIG. 8. Normalized radial profiles of the axisymmetric tangential winds at a height of 40 m AGL from 0133:37 to 0140:49 UTC. Also shown are a Rankine, modified Rankine, and Burgers–Rott vortex.

volume, 0134:23 UTC, the largest tangential velocities occurred at the lowest analysis level. During the next volumes, from 0135:20 to 01:36:49 UTC, the peak tangential velocities were located aloft (Fig. 7). By 0138:23 UTC, the maximum tangential velocity again peaked in the lowest analysis level and maintained a relatively steady value throughout the remainder of the analysis interval. The volumes during which the largest tangential velocities occurred aloft might have been an artifact of the temporal resolution of the radar; that is, the tornado may have been intensifying between successive scans. Throughout the domain, the maximum tangential velocities were located between the upward and downward branch of the two-celled vortex, similar to the observations of LW05 and KTW08.

Observations of tornadoes (LW05; KTW08) and hurricanes (Mallen et al. 2005) have yielded vortices that exhibit a modified Rankine vortex profile. Specifically, the tangential winds were observed to decay at a slower rate than r^{-1}. A decay coefficient α of 0.5–0.8 ($\alpha = 1$ for a Rankine vortex) was typical in the aforementioned studies. Similarly, in the Spencer tornado decay coefficients between 0.45 and 0.65 were calculated (Fig. 8). Smaller values of α suggest that more angular momentum was depleted as the flow spiraled inward, probably indicative of frictional dissipation. The value of α in the Spencer tornado did not show any discernable fluctuation as a function of intensity. As such, it is possible that the magnitude of the dissipation varied along the tornado's path (e.g., a change in surface roughness and/or debris loading) and/or another aspect of the flow superseded frictional dissipation. For example, surface roughness may have been substantially higher when the tornado crossed the town of Spencer from 0138 to 0139 UTC when Dowell et al. (2005) noted radar evidence of debris

loading. The findings of Lewellen et al. (1997, 2000) provide a mechanism that supports the latter assertion. Their results indicated that subsidiary vortices were an important mechanism for the inward transport of angular momentum, leading to a more intense vortex than was predicted by the initial boundary conditions. Indeed, Wurman (2002) found evidence of such vortices in the Spencer tornado at one observation time, but the vortices were not properly resolved with the DOW observations. Comparison of the tangential velocity profiles to an idealized Burgers–Rott vortex (BRV) based on the 0134:25 UTC wind field profile (Burgers 1948; Rott 1958) yielded a better match to the observations than a modified Rankine vortex. This is likely due to the inclusion of diffusion in the BRV, which balances the inward advection of angular momentum.

The properties of the air entering the tornado at low levels likely govern the low-level vortex dynamics (Lewellen et al. 2000). As a proxy for the environment immediately surrounding the tornado, the radial flow at a radius of 700 m (depicted by the black line in Fig. 6) gave some insight into the evolution of the tornado. Figure 9 depicts the radial wind at a radius of 700 m as a function of height within the lowest 400 m. As is evident, there was a markedly different distribution of winds as a function of time. Between 0133:37 and 0135:20 UTC, comparatively strong inflow of 10–20 m s^{-1} occurred very near the surface, below 250 m AGL. While the magnitude of this inflow decreased during this interval, inflow at 200 AGL decreased from 15.7 m s^{-1} at 0133:37 UTC to 7.7 m s^{-1} at 0134:23 UTC to 3.9 m s^{-1} at 0135:20 UTC, the change in radial winds with height within the lowest 200 m was comparatively less. After 0135:20 UTC, the low-level inflow decreased and was generally less than 6 m s^{-1} at all levels from 0136:01 through 0140:49 UTC. Aloft, at 400 m AGL (not shown), the evolution of inflow
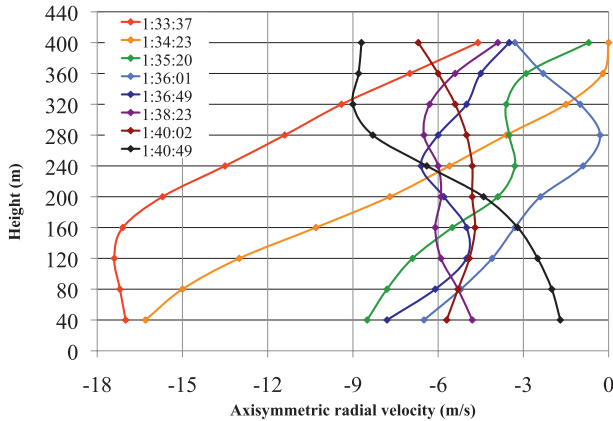
FIG. 9. The axisymmetric radial winds as a function of height at a radius of 700 m from 0133:37 to 0140:49 UTC. There is significant low-level inflow from 0133:37 to 0134:23 UTC, then weaker inflow through 0140 UTC and the end of the analysis period.

profiles was less systematic. Interestingly, the peak Doppler velocities occurred at 0136:52 UTC (Fig. 4a), following a local maximum in low-level radial wind profile. LW05 and KTW08 documented a similar relationship between tornado intensity and maxima in low-level radial inflow.

The influx of angular momentum into the tornado boundary layer is hypothesized to greatly impact low-level vortex dynamics (e.g., Lewellen et al. 2000; Lewellen and Lewellen 2007a,b). From 0133:37 through 0135:20 UTC, high-angular-momentum air was being transported inward (Fig. 10a). This transport occurred in tandem with the radial wind maximum, suggesting that the strength of the low-level secondary circulation and the low-level angular momentum transport were linked. Indeed, at

later times, when the low-level secondary circulation had weakened, the angular momentum transport had also weakened and occurred farther aloft (Fig. 10b). At early times, for example 0134:23 UTC in Fig. 10a, isopleths of axisymmetric angular momentum tilt inward with height. This suggests either that angular momentum is being depleted or that there are differences in advection of angular momentum by the mean winds at different altitudes. At later times, for example 0137:35 UTC, the isopleths are nearly vertical. This suggests that the previous factors are no longer present.

The swirl ratio S, a nondimensional parameter based on theoretical constructs, relates the swirling flow of a vortex to the inflow through a simple equation (Davies-Jones 1973; Rotunno 1979):

$$S = \frac{Rv_R}{2hu_R},$$

where R is the radius of the updraft, v_R is the average tangential velocity at the updraft radius, h is the depth of the inflow, and u_R is the average radial velocity at the updraft radius. Particular velocity configurations then correspond to a particular vortex structure. For $S > 1$, a two-celled structure and/or multiple vortices are predicted (Church et al. 1979). As mentioned previously, the Spencer tornado exhibited a two-celled structure throughout the duration of the GBVTD analysis. Additionally, the Doppler velocities suggested the presence of multiple vortices as was documented by Wurman (2002). Calculations of the swirl ratio for the Spencer tornado yielded values in excess of 1. It should be noted that because of an underrepresentation of the near-surface radial velocities in observations and consequently GBVTD-like
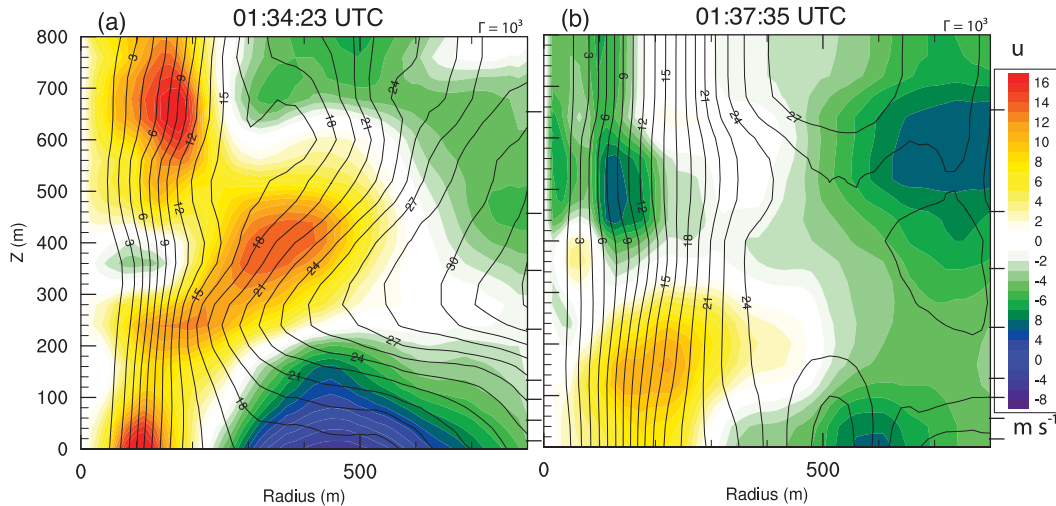

FIG. 10. Axisymmetric angular momentum (contours, 10^3 m^2 s^{-1}) and secondary circulation (shading) as a function of radius and height at (a) 0134:23 and (b) 0137:35 UTC.

retrievals, the swirl ratio might frequently be overestimated. However, the highest calculated swirl ratio, 7, occurred when the most prominent multiple vortices were observed, near 0135:20 UTC.

4. Summary and conclusions

The three-dimensional GBVTD analysis of the Spencer, South Dakota, tornado yielded a two-celled vortex structure throughout the duration of the 8-min observation period. Unlike the Kellerville (Wurman et al. 1996b), Dimmitt (Wurman and Gill 2000), and Harper (KTW08) tornadoes, changes in intensity did not correspond to any discernable changes in vortex morphology. At times, the inflow depth in Spencer was slightly less than the 600-m inflow of the Mulhall, Oklahoma, tornado but, similarly, the most intense inflow was confined to very near the surface. Although observations early in the analysis period revealed the presence of a radial jet, after 0136:01 UTC the low-level jetlike inflow was no longer discernable. This may be due in part to a change in turbulence intensity, which could occur with changes in surface roughness, shear profiles, etc., decreasing the tornado boundary layer thickness to levels below that which was observable. Intensification of the tornado vortex was preceded by surges of inflow in the lowest levels as also observed in LW05 and KTW08, bolstering the hypothesized link between increases in vortex intensity and increased low-level inflow, which could supply the vortex with transient increased fluxes of angular momentum. In particular, the secondary circulation may have been critical to inward transport of higher- angular-momentum air, against the dissipating effects of friction. Further, the largest axisymmetric tangential winds frequently occurred in the analysis level (40 m AGL), which is likely within or near the top of the boundary layer, perhaps also indicative of the effects of the radial jet on inward momentum transport.

The retrieved axisymmetric tangential winds were less intense than the peak Doppler winds (Fig. 3a). This was particularly true when multiple vortices were present, likely indicative of the large amount of energy contained in the asymmetries. Indeed, Lewellen et al. (1997) attribute additional inward transport of angular momentum to the presence of subsidiary vortices. In the present case, it was not possible to diagnose whether or not these vortices were instrumental in maintaining vortex intensity. Times with multiple vortices corresponded to higher swirl ratio values, corroborating conceptual models of tornado structure.

REFERENCES

Alexander, C. R., and J. Wurman, 2005: The 30 May 1998 Spencer, South Dakota, storm. Part I: The evolution and environment of the tornadoes. *Mon. Wea. Rev.,* **133,** 72–97.

——, and ——, 2008: Updated mobile radar climatology of supercell tornado structures and dynamics. *Extended Abstracts, 24th Conf. on Severe Local Storms,* Savannah, GA, Amer. Meteor. Soc., 19.4. [Available online at http://ams.confex.com/ams/24SLS/techprogram/paper_141821.htm.]

Bluestein, H. B., and W. P. Unruh, 1993: On the use of a portable FM-CW Doppler radar for tornado research. *The Tornado: Its Structure, Dynamics, Predication, and Hazards, Geophys. Monogr.,* Vol. 79, Amer. Geophys. Union, 367–376.

——, and A. L. Pazmany, 2000: Observations of tornadoes and other convective phenomena with a mobile 3-mm wavelength Doppler radar: The spring 1999 field experiment. *Bull. Amer. Meteor. Soc.,* **81,** 2939–2951.

——, A. L. Pazmany, J. C. Galloway, and R. E. Mcintosh, 1995: Studies of the substructure of severe convective storms using a mobile 3-mm-wavelength Doppler radar. *Bull. Amer. Meteor. Soc.,* **76,** 2155–2169.

——, W.-C. Lee, M. Bell, C. C. Weiss, and A. L. Pazmany, 2003: Mobile Doppler radar observations of a tornado in a supercell near Bassett, Nebraska, on 5 June 1999. Part II: Tornado-vortex structure. *Mon. Wea. Rev.,* **131,** 2968–2984.

——, C. C. Weiss, and A. L. Pazmany, 2004: The vertical structure of a tornado near Happy, Texas, on 5 May 2002: High-resolution, mobile, W-band, Doppler radar observations. *Mon. Wea. Rev.,* **132,** 2325–2337.

——, M. M. French, E. M. Holthaus, R. L. Tanamachi, S. Frasier, and A. L. Pazmany, 2007: The structure of tornadoes near Attica, Kansas, on 12 May 2004: High-resolution, mobile, Doppler radar observations. *Mon. Wea. Rev.,* **135,** 475–506.

Burgers, J. M., 1948: A mathematical model illustrating the theory of turbulence. *Adv. Appl. Mech.,* **1,** 197–199.

Church, C. R., and J. T. Snow, 1993: Laboratory models of tornadoes. *The Tornado: Its Structure, Dynamics, Predication, and Hazards, Geophys. Monogr.,* Vol. 79, Amer. Geophys. Union, 277–295.

——, ——, G. L. Baker, and E. M. Agee, 1979: Characteristics of tornado-like vortices as a function of swirl ratio: A laboratory investigation. *J. Atmos. Sci.,* **36,** 1755–1766.

Davies-Jones, R. P., 1973: The dependence of core radius on swirl ratio in a tornado simulator. *J. Atmos. Sci.,* **30,** 1427–1430.

——, 1976: Laboratory simulations of tornadoes. *Proc. Symp. on Tornadoes: Assessment of Knowledge and Implications for Man,* Lubbock, TX, Texas Tech University, 151–174.

——, 1986: Tornado dynamics. *Thunderstorms: A Social, Scientific and Technological Documentary,* Vol. 2, Thunderstorm Morphology and Dynamics, E. Kessler, Ed., University of Oklahoma Press, 197–236.

Dowell, D. C., Y. Richardson, and J. Wurman, 2002: Observations of the formation of low-level rotation: The 5 June 2001 Sumner County, Kansas, tornado. Preprints, *21st Conf. on Severe Local Storms,* San Antonio, TX, Amer. Meteor. Soc., 12.3. [Available online at http://ams.confex.com/ams/pdfpapers/47335.pdf.]

——, C. R. Alexander, J. M. Wurman, and L. J. Wicker, 2005: Centrifuging of hydrometeors and debris in tornadoes: Radar-reflectivity patterns and wind-measurement errors. *Mon. Wea. Rev.,* **133,** 1501–1524.

Fiedler, B. H., 1993: Numerical simulations of axisymmetric tornadogenesis in forced convection. *The Tornado: Its Structure, Dynamics, Predication, and Hazards, Geophys. Monogr.,* Vol. 79, Amer. Geophys. Union, 41–48.

——, and R. Rotunno, 1986: A theory for the maximum wind speeds in tornado-like vortices. *J. Atmos. Sci.,* **43,** 2328–2340.

Gall, R. L., 1983: A linear analysis of the multiple vortex phenomenon in simulated tornadoes. *J. Atmos. Sci.,* **40,** 2010–2024.

Howells, P. A. C., R. Rotunno, and R. K. Smith, 1988: A comparative study of atmospheric and laboratory-analogue numerical tornado vortex models. *Quart. J. Roy. Meteor. Soc.,* **114,** 801–822.

Kosiba, K. A., R. J. Trapp, and J. Wurman, 2008: An analysis of the axisymmetric three-dimensional low level wind field in a tornado using mobile radar observations. *Geophys. Res. Lett.,* **35,** L05805, doi:10.1029/2007GL031851.

Lee, W.-C., and J. Wurman, 2005: Diagnosed three-dimensional axisymmetric structure of the Mulhall tornado on 3 May 1999. *J. Atmos. Sci.,* **62,** 2373–2393.

——, B. J.-D. Jou, P.-L. Chang, and S.-M. Deng, 1999: Tropical cyclone kinematic structure retrieved from single-Doppler radar observations. Part I: Interpretation of Doppler velocity patterns and the GBVTD technique. *Mon. Wea. Rev.,* **127,** 2419–2439.

Lewellen, D. C., and W. S. Lewellen, 2007a: Near-surface intensification of tornado vortices. *J. Atmos. Sci.,* **64,** 2176–2194.

——, and ——, 2007b: Near-surface vortex intensification through corner flow collapse. *J. Atmos. Sci.,* **64,** 2195–2209.

——, ——, and J. Xia, 2000: The influence of a local swirl ratio on tornado intensification near the surface. *J. Atmos. Sci.,* **57,** 527–544.

Lewellen, W. S., and Y. P. Sheng, 1980: Modeling tornado dynamics. U.S. Nuclear Regulation Committee Rep. NUREG/CR-2585, 227 pp.

——, D. C. Lewellen, and R. I. Sykes, 1997: Large-eddy simulation of a tornado's interaction with the surface. *J. Atmos. Sci.,* **54,** 581–605.

Mallen, K. J., M. T. Montgomery, and B. Wang, 2005: Reexamining the near-core radial structure of the tropical cyclone primary circulation: Implications for vortex resiliency. *J. Atmos. Sci.,* **62,** 408–425.

Marquis, J., Y. Richardson, J. Wurman, and P. Markowski, 2008: Single- and dual-Doppler analysis of a tornadic vortex and surrounding storm-scale flow in the Crowell, Texas, supercell of 30 April 2000. *Mon. Wea. Rev.,* **136,** 5017–5043.

Mohr, C. G., L. J. Miller, R. L. Vaughn, and H. W. Frank, 1986: Merger of mesoscale datasets into a common Cartesian format for efficient and systematic analyses. *J. Atmos. Oceanic Technol.,* **3,** 143–161.

Richardson, Y., D. Dowell, and J. Wurman, 2001: High resolution dual-Doppler analyses of two thunderstorms during the pretornadogenesis and mature tornado stages. Preprints, *30th Int. Conf. on Radar Meteorology,* Munich, Germany, Amer. Meteor. Soc., 295–297.

Rott, N., 1958: On the viscous core of a line vortex. *Z. Angew. Math. Phys.,* **9,** 543–553.

Rotunno, R., 1977: Numerical simulation of a laboratory vortex. *J. Atmos. Sci.,* **34,** 1942–1956.

——, 1979: A study in tornado-like vortex dynamics. *J. Atmos. Sci.,* **36,** 140–155.

——, 1984: An investigation of a three-dimensional asymmetric vortex. *J. Atmos. Sci.,* **41,** 283–298.

Tanamachi, R. L., H. B. Bluestein, W. C. Lee, M. Bell, and A. L. Pazmany, 2007: Ground-based velocity track display (GBVTD) analysis of W-band Doppler radar data in a tornado near Stockton, Kansas on 15 May 1999. *Mon. Wea. Rev.,* **135,** 783–800.

Walko, R. L., 1988: Plausibility of substantial dry adiabatic subsidence in a tornado core. *J. Atmos. Sci.,* **45,** 2251–2267.

Ward, N. B., 1972: The exploration of certain features of tornado dynamics using a laboratory model. *J. Atmos. Sci.,* **29,** 1194–1204.

Wurman, J., 2001: The DOW mobile multiple-Doppler network. Preprints, *30th Conf. on Radar Meteorology,* Munich, Germany, Amer. Meteor. Soc., 95–97.

——, 2002: The multiple vortex structure of a tornado. *Wea. Forecasting,* **17,** 473–505.

——, and S. Gill, 2000: Finescale radar observations of the Dimmitt, Texas (2 June 1995), tornado. *Mon. Wea. Rev.,* **128,** 2135–2164.

——, and C. R. Alexander, 2005: The 30 May 1998 Spencer, South Dakota, storm. Part II: Comparison of observed damage and radar-derived winds in the tornadoes. *Mon. Wea. Rev.,* **113,** 97–119.

——, J. Straka, and E. Rasmussen, 1996a: Fine-scale Doppler radar observation of tornadoes. *Science,* **272,** 1774–1777.

——, ——, and ——, 1996b: Preliminary radar observations of the structure of tornadoes. Preprints, *Conf. on Severe Local Storms,* San Francisco, CA, Amer. Meteor. Soc., 17–22.

——, ——, ——, M. Randall, and A. Zahrai, 1997: Design and deployment of a portable, pencil-beam, pulsed, 3-cm Doppler radar. *J. Atmos. Oceanic Technol.,* **14,** 1502–1512.

——, Y. Richardson, C. Alexander, S. Weygandt, and P. F. Zhang, 2007a: Dual-Doppler and single-Doppler analysis of a tornadic storm undergoing mergers and repeated tornadogenesis. *Mon. Wea. Rev.,* **135,** 736–758.

——, ——, ——, ——, and ——, 2007b: Dual-Doppler analysis of winds and vorticity budget terms near a tornado. *Mon. Wea. Rev.,* **135,** 2392–2405.

——, C. Alexander, Y. P. Richardson, P. Robinson, and W. Lee, 2008: GBVTD analysis of the Spencer, South Dakota (1998) tornado. Preprints, *24th Conf. on Severe Local Storms,* Savannah, GA, Amer. Meteor. Soc., P13.7. [Available online at http://ams.confex.com/ams/24SLS/techprogram/paper_142181.htm.]

——, K. A. Kosiba, P. Markowski, Y. Richardson, and P. Robinson, 2010: Fine-scale single- and dual-Doppler analysis of tornado intensification, maintenance, and dissipation in the Orleans, Nebraska, tornadic supercell. *Mon. Wea. Rev.,* in press.

CORRIGENDUM

KAREN KOSIBA AND JOSHUA WURMAN

Center for Severe Weather Research, Boulder, Colorado

In Kosiba and Wurman (2010), the authors failed to include an important acknowledgment. The following sentence should have been included in the Acknowledgments section: ''The authors acknowledge the support of National Science Foundation Grants 0801041, 0734001, and 0724318.''

REFERENCE

Kosiba, K., and J. Wurman, 2010: The three-dimensional axisymmetric wind field structure of the Spencer, South Dakota, 1998 tornado. *J. Atmos. Sci.,* **67,** 3074–3083.

Corresponding author address: Karen Kosiba, Center for Severe Weather Research, 1945 Vassar Circle, Boulder, CO 80305.
E-mail: kakosiba@cswr.org